NCREE NEWSLETTER

June 2013 VOL. 8 NO. 2



CONTENTS

- Centrifuge Shaking Table Tests on the Seismic Responses of Geosynthetic Reinforced Earth Embankments
- Foundation Inspection of the Old Jhong-Jheng Bridge in Hsinchu
- Testing and Analysis of a Laterally Loaded Model Pile
- Shaking Table Test on a Model Pile in Saturated Sloping Ground
- The March 27, 2013 M_L-6.2 Renai Earthquake in Taiwan
- IDEERS 2013

DIRECTOR

Kuo-Chun Chang

EDITORS

Jiunn-Shyang Chiou

Yung-Yen Ko

National Center for Research on Earthquake Engineering

Centrifuge Shaking Table Tests on the Seismic Responses of Geosynthetic Reinforced Earth Embankments

Wen-Yi Hung, Associate Technologist, NCREE
Jin-Hung Hwang, Chung-Jung Lee, National Central University

Reinforced earth structures are generally constructed of backfill and manufactured materials, such as metal strips and geosynthetic sheets or grids, known as reinforcements. These reinforcements sustain the forces resulting from the deformation of reinforced earth structures and external loadings. The biggest advantage of reinforced earth structures over reinforced concrete structures is their flexibility and capacity to absorb deformations due to poor foundations and seismic loadings. In this research, five centrifuge models were performed in a 50 g acceleration field to investigate the effects of the reinforcement on the seismic response of geosynthetic reinforced earth (GRE) embankments, including the natural frequency and the amplification of acceleration. Table 1 shows the characteristics of the models. Figure 1 shows the top view of model GREE5 after construction. Seven accelerometers were installed on each model, including one fixed onto the shaking table to monitor the input motion, and two accelerometer arrays instrumented inside the retained soil zone and inside the reinforced earth zone. Eight linear variable differential transformers were placed on the model to measure the settlement on top of the embankment and the horizontal displacement of the facing.

From the test results, it was found that the natural frequency for all the GRE models was about 5.7 Hz, indicating that the reinforcement spacing and the face inclination did not affect the natural frequency of the GRE embankment. The natural frequency of an 8-m-high embankment is therefore about 5.7 Hz. On the other hand, the transfer functions at input motions of 1 Hz for different elevations were close to 1, illustrating that the acceleration was not amplified. At input motions of 4.8 Hz, significantly different values of transfer functions were observed, leading to different amplifications of acceleration at varying elevations. In the following section, the amplifications of the accelerations are calculated directly from the acceleration responses of different seismic events.

The measurements of each seismic event were divided into the responses of the retained soil zone and of the reinforced earth zone, as shown in Figure 2. The two figures show the relationship between the elevation normalized by height and the mean values of the amplification, where the hollow and solid symbols are graded into input motions with a frequency of 1 Hz and 4.8 Hz, respectively. For each frequency of input motion, there are three different related base input accelerations: small, medium, and large accelerations labeled in the figures as circles, squares, and triangles, respectively.

It can be seen that the mean amplification increases slightly with increasing elevation. The maximum amplification was found to be about 1.3 at the top of the retained soil zone for an 8-m-high GRE embankment subjected to 1 Hz at a small seismic loading. On the other hand, the mean amplification increased dramatically with increasing elevation when the input motion frequency was raised to 4.8 Hz. The maximum amplification of acceleration at the top of the embankment was more than about 5.5. Consequently, if a constant amplification of acceleration is used to design a GRE embankment, the results would underestimate the seismic behavior of the top portion of the GRE embankment, as the frequency of the input motion is close to the natural frequency of the system.

Table 1 The characteristics of GRE embankment models

No.	Width (m)	Height (m)	Slope	s_v (m)	T_u (kN/m)
GREE4	18.35	8.0	1:1.0	0.8	112.0
GREE5	18.35	8.0	1:0.5	0.8	112.0
GREE6	18.35	8.0	1:0.5	0.8	62.5
GREE8	18.35	8.0	1:1.0	0.5	112.0
GREE9	18.35	8.0	1:0.5	0.5	112.0

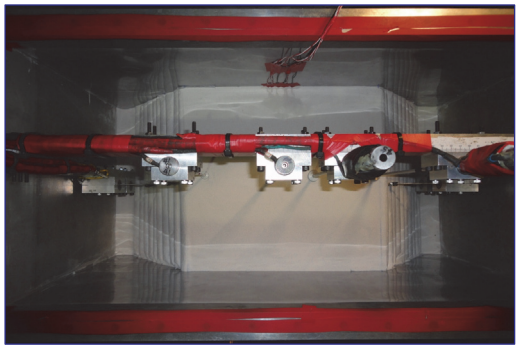


Fig. 1 the top view of model GREE5 after construction

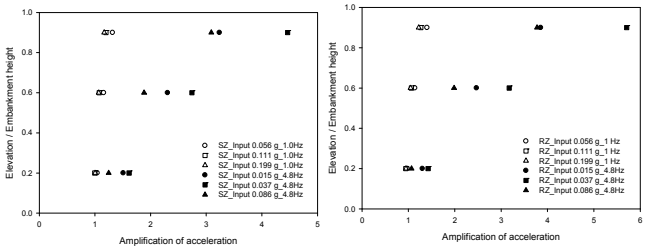


Fig. 2 The amplification of acceleration for different input motions inside (left) the retained soil zone; and (right) inside the reinforced zone

(Yu-Wen Chang, ywchang@ncree.narl.org.tw)

Foundation Inspection of the Old Jhong-Jheng Bridge in Hsinchu

Yung-Yen Ko, Associate Research Fellow, NCREE

Introduction

The old Jhong-Jheng Bridge in Hsinchu crosses the Tou-Cian River. Scouring and erosion have formed many gullies on the riverbed, causing several of the bridge piers to suffer foundation exposure. The strong current induced by the heavy rainfall of Typhoon Saola in 2012 severely exposed the caisson foundation of pier P9, as shown in Fig. 1. Due to structural instability, this bridge has been closed, and a new bridge is set to be constructed. Taking advantage of the closure, microtremor measurements were made to investigate the influence of foundation exposure on the dynamic behavior of the bridge. In addition, the impulse response method was utilized to examine the length of the caisson foundation.



Fig. 1 Scour condition of the old Jhong-Jheng Bridge

Microtremor Measurement

During the period when the old Jhong-Jheng Bridge was closed, a microtremor measurement was conducted on its superstructure. The measuring points were located at pier P9, where the foundation exposure was the most severe, and at neighboring piers P10 and P11, as shown in Fig. 1. Velocity-type vibro-sensors were adopted and installed on the deck. When the measurement was performed, the exposed depth of the caisson of pier P9 was estimated at around 15 m using a plumb bob and measuring tape.

Fig. 2 shows the average Fourier spectra of the horizontal transverse vibrations (parallel to the flow direction). Most of the vibrations at piers P10 and P11 are concentrated in a frequency range of 2–4 Hz, with predominant frequencies of 2.8 Hz and 3.3 Hz, respectively. For pier P9, an obvious peak is noted at 1.5 Hz. The predominant frequency of P10 is found to be lower than that of P11, where the protective works remained intact, probably because the protective work of P10 was partially damaged. Meanwhile, pier P9, which suffered severe scouring, has a lower predominant frequency than both P10 and P11. Therefore, the exposure of the foundation appears to cause the predominant frequency of vibration of the pier to be decreased.

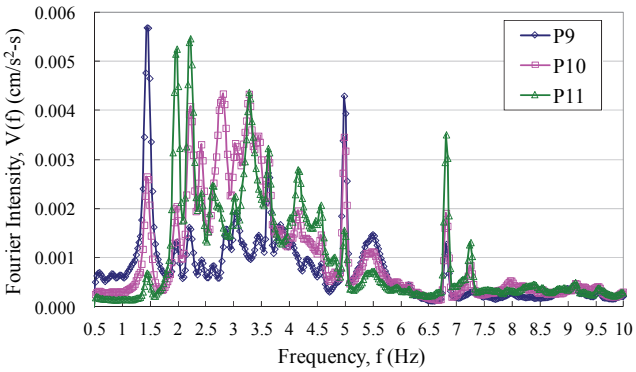


Fig. 2 Average Fourier spectra of the microtremor responses of piers P9~P11

Impulse Response Testing

The caisson foundation was used for the construction of the old Jhong-Jheng Bridge. However, the design drawings are unavailable and, thus, the foundation depth is unknown. Therefore, the impulse response method was adopted for the caisson length of pier P11. The caisson top was impacted by an impulse hammer, inducing a transient impulse that propagated downward along the caisson wall. When the impulse reached the bottom of the caisson, reflection occurred. Accelerometers were installed on the top of the caisson to measure the propagation of the impulse waves. The travelling distance of the impulse can be calculated by the time lag between the incident and reflected waves passing the caisson top and the P-wave velocity in the caisson wall. Thus, the caisson length can be deduced.

Fig. 3 gives the time history of the impulse response at the top of the caisson. The waveforms of the incident and reflected waves are identifiable. A representative travelling duration of the impulse, 1.053×10^{-2} s, was obtained, and the P-wave velocity was estimated to be around 4975 m/s. From this, the caisson length can be calculated to be about 26.2 m. As mentioned, the exposed depth of the P9 caisson was close to 15 m. If the length of the P9 caisson is the same as that of P11, then the exposure exceeds half of the caisson length. Therefore, the foundation stability of pier P9 might be insufficient..

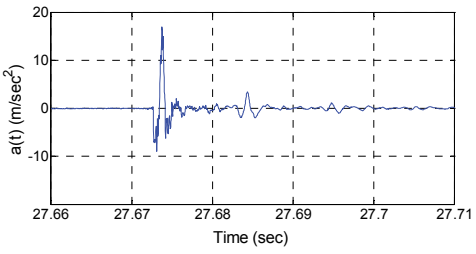


Fig. 3 Impulse response on the top of P11 caisson

(Yung-Yen Ko, yyko@ncree.narl.org.tw)

Testing and Analysis of a Laterally Loaded Model Pile

Jiunn-Shyang Chiou, Research Fellow, Chia-Han Chen, Assistant Research Fellow, NCREE
Wei-Lun Tai, National Taiwan University

The loading history–dependent unloading–reloading response is a major feature of the lateral behavior of piles under repetitive loading. The enclosed loop of hysteresis provides a mechanism for energy dissipation to reduce the pile's response to dynamic loading. With the development of performance-based design, the magnitude of residual displacement is an important index for checking the structural functionality of a pile and, therefore, a complete tracing of the locus of loading–unloading–reloading is necessary. To understand the hysteretic behavior of a laterally loaded pile, this study conducted pushover tests on a model pile at the National Center for Research on Earthquake Engineering (NCREE) of Taiwan.

The model pile-–soil system is shown in Fig. 1. The model pile was an aluminum pipe of outer diameter 101.6 mm, thickness 3 mm, and length 1.6 m. A 1.35 -m-thick Vietnam sand specimen was prepared in a test box. The relative density of the soil specimen was about 25.6% (loose sand). The tip of the pile was fixed at the bottom of the box and the actuators used to push the pile were displacement controlled Two successive tests were conducted. Tests Y-1 and Y-2 were loaded in the *y*-direction with target displacements of 5 mm and 10 mm, respectively. Each test had one displacement cycle containing both positive and negative directions of movement. Fig. 2 shows the load–deflection curves for all the tests. The load–deflection curves showed a significant loop of hysteresis: the effective damping ratios for lateral displacements of 5 mm and 10 mm were about 25% and 32–34%, respectively.



Fig.1 The model for the pushover tests

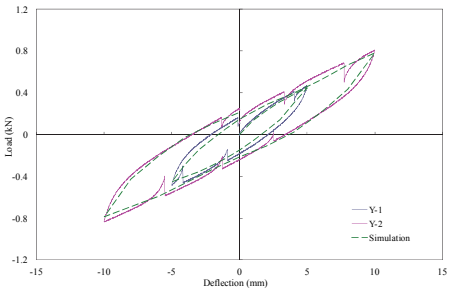


Fig.2 The load-deflection curves

According to the beam theory, the pile displacement profiles were obtained by integrating the curvature functions twice, while the soil reaction distributions were computed by differentiating the moment curves twice. Collecting soil reaction and pile displacement distributions gave the *p*–*y* curves for each test.

Two elements are used to describe the complete locus of the experimental *p*–*y* curves: (1) a backbone curve and (2) a restoring force model. The secant slope of the backbone curves (*i.e.*, the subgrade reaction modulus) is a function of depth and displacement. Using a common reference for comparison, a reference displacement y_{ref} is set to be 0.01 pile diameter, that is y_{ref} =1 mm. For each depth, the secant subgrade reaction modulus at y_{ref}, Es_{ref}, was computed and the relationship of Es_{ref} versus depth was constructed, as shown in Fig. 3, demonstrating that an approximately linear relationship of Es_{ref} versus depth. In addition, as shown in Fig. 4, the ratio of Es/Es_{ref} decreased with the ratio of y/y_{ref} with an order of about −0.5.

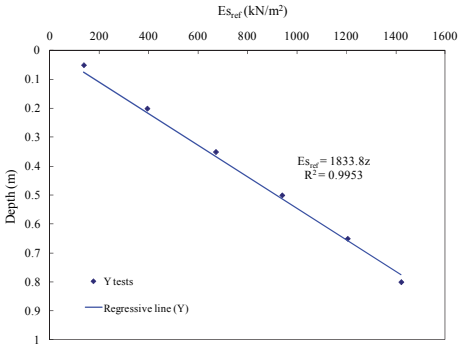


Fig. 3 Plots of Es_{ref} versus depth

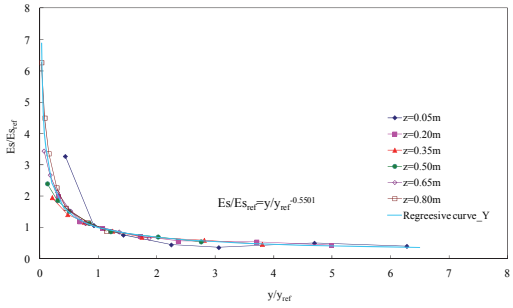


Fig. 4 Plots of Es/Es_{ref} versus y/y_{ref}

To trace the locus of the *p*–*y* loop, a simple restoring force model of the Masing type was examined. The nonlinear pushover simulations were performed using SAP2000. The results are displayed in Fig. 2 and indicate that the pushover curves from the analysis were in good agreement with the experimental ones.

(Jiunn-Shyang Chiou, jschiou@ncree.narl.org.tw)

Shaking Table Test on a Model Pile in Saturated Sloping Ground

Chia-Han Chen, Assistant Research Fellow, NCREE
Tzou-Shin Uneg and Cheng-Hsing Chen, National Taiwan University

Pile foundations have suffered extensive damages within liquefiable and laterally spreading ground in many large earthquakes. Therefore, it is necessary to investigate the mechanism of lateral spreading and its effect on the structure for the mitigation of liquefaction-induced damages and to provide information of performance criteria for the seismic design of foundations.

In this study, shaking table tests on a model pile in an inclined large biaxial laminar shear box filled with saturated clean sand were conducted at the National Center for Research on Earthquake Engineering (NCREE), Taiwan. The model pile was made of an aluminum alloy pipe, and its tip was vertically fixed at the bottom of the shear box to simulate the condition of a pile foundation embedded in a firm stratum. The pile top was mounted with six steel disks to simulate the superstructure. The shear box was inclined 2° to the horizontal, simulating a mild infinite slope. The sloping direction of this model was in the x-direction, as shown in Figure 1.

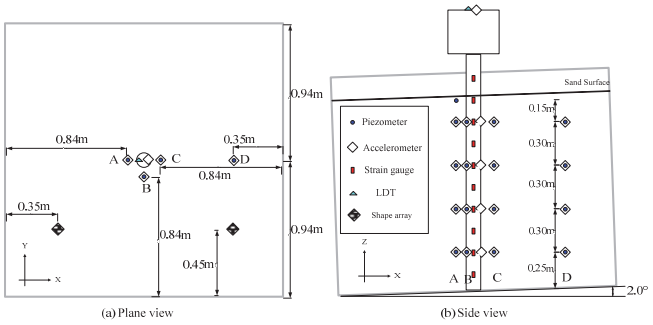


Fig.1 Instrumentation on the pile and within the sand specimen

Input motions were mainly imposed perpendicularly to the slope direction to study of the kinematic effect on the pile foundation independently. Tests also carried out in a direction parallel to the slope to investigate the resultant force on the pile foundation, including the inertial and kinematic effects. Strain gauges and accelerometers were placed on the pile surface to obtain the response of the pile under shaking. The near-field and far-field soil responses, including pore water pressure changes, accelerations, and settlements were also measured. The soil and pile responses and their interaction, including the inertial and kinematic actions on the model pile, under these types of shakings were studied.

A shaking table test under one-dimensional sinusoidal acceleration with a frequency of 8 Hz and an amplitude of 0.068 g in the y-direction was conducted to study the kinematic effect on the pile foundation in a saturated sloping ground with relative density of 13.6%. In this test, the liquefied depth of the sand specimen reached about 112.6 cm. Figure 2 shows a distinct lateral spreading displacement after the shaking.

The time histories of relative displacement of the pile top are shown in Figure 3. The x-displacement of the model pile is mainly caused by lateral spreading, and the displacement in the other direction is induced by the shaking. Hence, the force exerted on the model pile due to lateral spreading (x-direction) can be extracted from this type of test. It was also observed that the pile response demonstrated a free vibration motion at 4.2 to 8 seconds. The predominant frequency of the acceleration on the pile top in the x-direction is about 2 Hz. By comparing this result with the predominant frequency of the model pile without the soil specimen, one can find that the predominant frequency of the model pile within liquefied soil was almost the same as that of the model pile without the soil specimen. This inferred that the stiffness of the soil had almost completely dissipated when soil liquefaction occurred.



Fig.2 Liquefaction-induced lateral spreading displacement in the x-direction

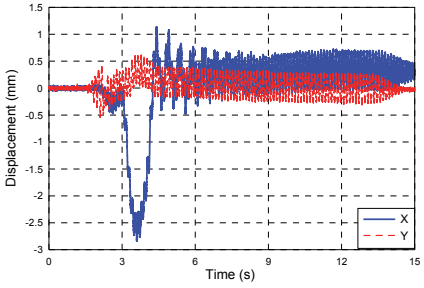


Fig.3 The time histories of the relative displacement of the pile top

Shaking table tests were conducted on an aluminum model pile in saturated sloping ground using the biaxial laminar shear box. Analyses of the dynamic behavior of the model pile and the soil stratum were conducted during the shaking tests according to observations. The lateral spreading displacements of the soil and pile behaviors were observed while soil liquefaction was triggered by the shaking. It was also found that the kinematic loading on the model pile due to lateral spreading during shaking could be separated individually in a suitable way by using the biaxial shear box. Further analyses of the test data will be performed to obtain more information on the relationship between the mobilized lateral pressure on the pile and the ground movement and the evaluation of the bending moment of the pile in design.

(Chia-Han Chen, chiaham@ncree.narl.org.tw)

The March 27, 2013 M_L-6.2 Renai Earthquake in Taiwan

On March 27, 2013, at 10:03:19.7 CST (02:03:19.7 UTC), an M_L 6.2 earthquake occurred in the mountainous area of Nantou in central Taiwan. According to the report (Fig. 1) from the Central Weather Bureau (CWB), the epicenter of the mainshock was located at 121.05° E and 23.9° N, about 38 km east of the Nantou County Hall. The focal depth was originally determined to be 15.4 km, but was revised down to 19.4 km. The moment magnitude M_W was 5.9 from the US Geological Survey (USGS); the location was 121.221 °E and 23.827 °N, and the focal depth was 21.4 km. This earthquake was felt all over Taiwan Island.

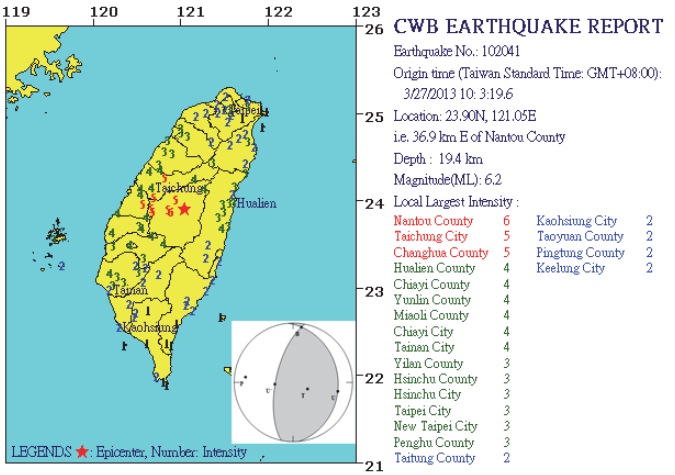


Fig. 1 The report of the 0327 earthquake

The focal mechanisms calculated in institutes in Taiwan and the U.S. are very similar. This report uses the Centroid Moment Tensor solution from the CWB, as shown in Fig. 1. According to the distribution of aftershocks and the tectonic setting near the hypocenter, we believe that the strike angle of the real fault-plane solution was 355°, with a dip angle of 25° to the east, and slipped along a rake of 75°. More than 500 aftershocks occurred within the two days after the mainshock; the largest magnitude aftershock was only M_L = 5.0, to the northwest of the mainshock.

According to the earthquake report, the real-time strong ground motion Station SML had the largest recorded PGA of 282.27 gal in the east–west direction. The ground shaking level was CWB-defined Intensity 6 (PGA 250–400 gal) at this station. The shaking intensities at other regions in Taiwan were as shown in Fig. 1. After the recordings of the free-field strong motion stations in central Taiwan became available, they showed that three stations recorded very strong peak ground accelerations of more than 400 gal (CWB Intensity 7). These stations are TCU142 (488.20 gal), TCU143 (445.64 gal), and TCU148 (483.40 gal) with epicentral distances of 19.9 km, 29.8 km, and 13.42 km, respectively. Moreover, these stations are all to the west of the epicenter and the PGAs are all in the east–west direction. We speculate that this may be due to the fault plane solution and the radiation pattern of the S-wave.

Damage to Buildings

Several buildings were damaged in the Taichung and Nantou areas by the earthquake. An investigation team organized by NCREE investigated sixteen buildings, including private buildings, temples, government offices, and public buildings. No buildings collapsed during this earthquake. Most of the damage to the buildings involved non-structural masonry walls, whereas major structural components showed no damage. The following section covers the seriously damaged buildings.

As shown in Fig. 2, the Dali Jinghua building was a ten-story reinforced concrete (RC) building in Taichung city, and it was damaged by punch cracks with an expansion gap between two major structures. As shown in Figs. 3 and 4, the Deyi Zhiji building was a twelve-story RC building in Taichung city, and the RC wall of the mechanical parking tower and first floor were damaged. As shown in Fig. 5, the Yuchih township office was a four-story RC building, and damage occurred in the RC walls beside windows with shear cracks.

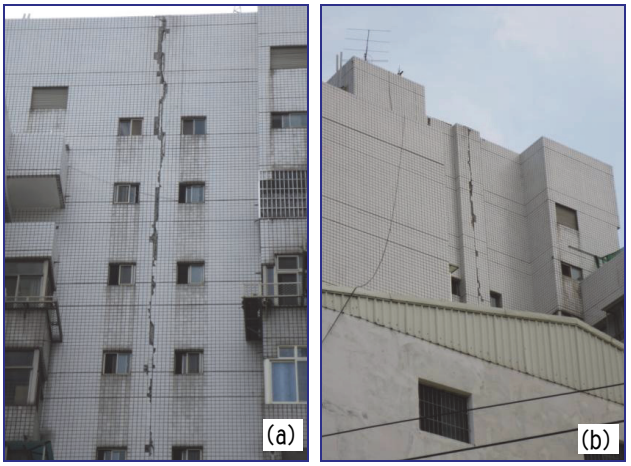


Fig. 2 The punch cracks with an expansion gap in the Dali Jinghua building in Taichung: (a) north side and (b) south side

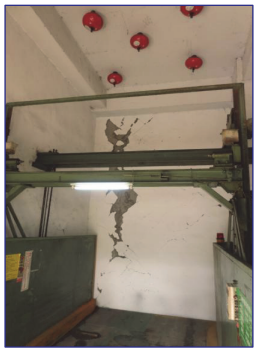




Fig. 4 The horizontal cracks of the first floor of the Deyi Zhiji building in Taichung

Fig. 3 The vertical cracks in the RC wall of the mechanical parking tower of the Deyi Zhiji building in Taichung



Fig. 5 The shear cracks beside the windows in the RC wall of the Yuchih township office in Nantou County

Damage of School Buildings

The main damaging effects of the earthquake were concentrated on school buildings in Taichung City, Changhua County, and Nantou County. The NCREE received damage information for these school buildings from the government, and these were prioritized for reconnaissance according to this information. A reconnaissance team from the NCREE was organized and sent to the affected area to carry out detailed investigations of the damage to school buildings.

The damage to school buildings can be separated into structural and nonstructural, respectively. Even so, the structural damage was light. The structural damage was split along the interfaces between the beam and brick walls. Fig. 6 shows the out-of-plane deformation that occurred on the brick wall. In addition, there was obvious shear failure on the partition wall, as shown in Fig. 7. In the damaged school buildings, a shear crack was found on the short column and beam. The typical shear failure is clearly visible in Fig. 8. Typical nonstructural damage involved suspended ceilings and could be observed in several schools. The major damage to suspended ceilings occurred around the perimeter adjacent to the structure (Fig. 9). Other damage was caused by collisions due to insufficient distance between adjacent school buildings. Fig. 10 shows the visible failure on the adjacent columns.



Fig. 6 Out-of-plane deformation occurring on a brick wall



Fig. 7 Shear crack occurring on the brick wall of a junior high school



Fig. 8 Shear crack on a beam due to the short beam effect

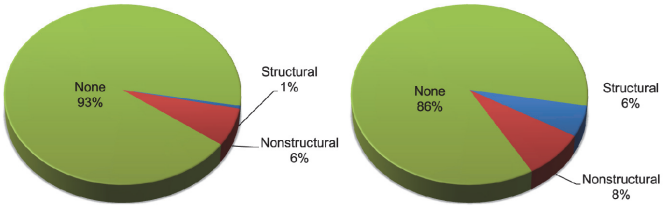


Fig. 9 Damaged suspended ceilings in the activity center of an elementary school



Fig. 10 Two buildings that collided against one another during the earthquake

We were concerned about the damage to school buildings where retrofitting measures had already been constructed. Measurements relating to the classification of damage were carried out. In Fig. 11(a), the percentage of structural damage is only 1% for schools having been retrofitted, but the percentage of structural damage rises to 6% for schools not yet retrofitted, as shown in Fig. 11(b). More details are shown in Fig. 11.



(a) Accomplished (b) Unaccomplished

Fig. 11 Statistics of the classification of damage to school buildings

The earthquake caused structural damage to many school buildings, but the main damage occurred along the interfaces between the beams and walls. Although this damage will not compromise the structure, rain might leak through the cracks. On the other hand, some school buildings collided against one another due to the insufficient distance between two buildings. This issue of collision should be considered in seismic design, for instance, by increasing the distance between buildings to prevent such damage from occurring again. However, the situation of each school building is quite different, so therefore the engineer should deliver the best solution on a case-by-case basis.

Damage of Nonstructural Components and Systems

A damage survey of nonstructural components and systems was conducted on March 28th, 2013, by the NCREE on the public facilities located in the seismically affected area. This reconnaissance report summarizes the major nonstructural damage to the County Hall of the Nantou County Government

(CHNCG), the Office Building of the Health Bureau (OBHB) of the Nantou County Government, and the Building of the National Chi Nan University Library (BNCNUL). In addition, as contributed by Prof. Chi-Chang Lin, non-structural damage in the National Chung Hsing University (NCHU) was also included in this report. It is noted that the buildings in these facilities remained structurally intact or sustained only minor damage.

Typical damage to nonstructural components and systems in these facilities involved the falling down of suspended ceilings and the overturning of freestanding cabinets and bookshelves. The major damage to ceilings occurred around the perimeter adjacent to the structures, where runners deformed and detached from moldings and ceiling panels fell off. In addition, one elevator in the CHNCG was shut down due to the deformation of the counterweight support component. In the OBHB, the floor tiles were uplifted, caused by racking deformation and penetrating cracks occurring on the partition walls. The HVAC (Heating, Ventilation and Air Conditioning) duct in the BNCNUL was damaged due to the large displacement of the ceiling system. In addition to the typical damage to bookshelves, the suspended ceiling system, and attached HVAC ducts, the cracks in partition walls, as well as the breaking of the piping system and glazed windows, in the NCHU, the adhered veneers also fell down due to unexpected drift during the earthquake.



Overturning of freestanding cabinet in CHNCG



Damage to suspended ceiling in OBHB



Falling of the suspended ceiling system in the BNCNUL



Overturning of freestanding bookshelves in the NCHU

Fig. 12 Seismic damage to nonstructural components and systems

Early Earthquake Warning System

The Early Earthquake Warning System (EEWS) installed at Gang Ping Elementary School in Chiayi City issued an earthquake alarm 13 sec before the strong S-wave arrival (Fig. 13), which demonstrated the effectiveness of the system through *in situ* applications. The school teachers and students were able to follow their training to evacuate classrooms with minimum panic.

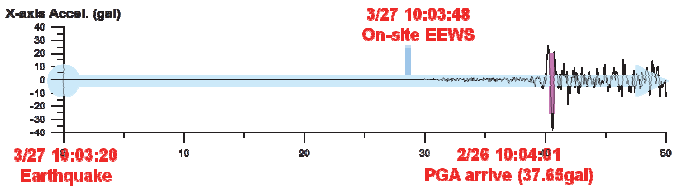


Fig. 13 The EEWS warning signal sequence at Gang Ping Elementary School.

Reconnaissance report prepared by: Juin-Fu Chai, Te-Kuang Chow, Tsung-Chih Chiou, Fu-Pei Hsiao, Shieh-Kung Huang, Chun-Hsiang Kuo, Zih-Yu Lai, Che-Min Lin, Fan-Ru Lin, Pei-Yang Lin, Zhen-Yu Lin, Wen-Cheng Shen, Pu-Wen Weng, Chiun-lin Wu.

IDEERS 2013

Mu-Hsuan Li, Assistant Technologist, NCREE

In order to encourage students' participation in science games and stimulate their creativity, an earthquake engineering education project, entitled "Introducing and Demonstrating Earthquake Engineering Research in Schools" (IDEERS), will be held by the National Center for Research on Earthquake Engineering (NCREE), the British council in Taipei, the National Science and Technology Center for Disaster Reduction (NCDR), and the National Applied Research Laboratories (NARL) on September 13–15.

IDEERS is a science-based project with a competition developed by the Earthquake Engineering Research Center of Bristol University. The target participants of the IDEERS competition are graduate and undergraduate students majoring in civil engineering–related subjects and high school students. Students entering the competition will make their models using cheap materials at the NCREE and have them tested on the "Tri-Axial Seismic Simulator" (or shaking table). Models will be shaken to destruction, and the best-designed models will win prizes.

For further information, please see the IDEERS web-site: http://w3.ncree.org/ideers/2013/.

Published by

National Center for Research on Earthquake Engineering

200, Sec. 3, XinHai Rd., Taipei 106, Taiwan, R.O.C.

Phone: 886-2-6630-0888

Fax: 886-2-6630-0858

Website: http://newsletter.ncree.org

The National Center for Research on Earthquake Engineering (NCREE) is a laboratory of National Applied Research Laboratories (NARL)

Website: http://www.narl.org.tw